STRUCTURAL AND DIPOLAR PROPERTIES OF THE VOLTAGE-DEPENDENT PORE FORMER ALAMETHICIN IN OCTANOL/DIOXANE

G. SCHWARZ AND P. SAVKO
Department of Biophysical Chemistry, Biocenter of the University of Basel, Switzerland

ABSTRACT Dielectric constant and loss of the membrane-active peptide alamethicin in octanol/dioxane mixtures have been measured at frequencies between 5 kHz and 50 MHz. On the basis of a rotational mechanism of dipolar orientation, the observed dispersion provides information regarding size, shape, and dipole moment of the structural entities which the solute may assume in media of diverse lipophilicity. Particularly detailed results are obtained in a pure octanol solvent where an apparent molecular weight of alamethicin could be determined. It turns out that in this quite lipophilic medium most of the peptide material exists as a monomer particle that has approximate length and diameter of 35 and 13 Å, respectively. It carries a dipole moment of ~75 Debye units (directed nearly parallel to the long axis). At our concentrations of a few milligrams per milliliters, appreciable formation of dimers by head-to-tail linkage is indicated. When the octanol content is reduced by adding greater amounts of dioxane, larger particles are encountered. This is accompanied by a decrease of the effective polarity. The inherent increase of hydrophilicity in the dioxane-enriched solvent apparently favors another monomer conformation that has a low dipole moment and easily aggregates to some kind of micelle.

1. INTRODUCTION

The peptide antibiotic alamethicin has been shown to induce ionic permeabilty of membranes by pore formation (1, 2). Because this process exhibits a substantial dependence on the electric potential across the membrane, it has attracted great interest as a model for the phenomenologically similar behavior of ionic channels in nerve membranes (3).

So far the underlying molecular mechanisms of such voltage-dependent events in membranes are still a matter of speculation. In particular, one does not know the actual nature of the critical step in pore activation that is directly controlled by the electric field in the membrane.

There is, however, good reason to believe that this involves a transition between states of different macromolecular structures. If such a reaction is associated with a sufficient change of dipole moment it follows from fundamental thermodynamic principles that the structural equilibrium will indeed be considerably displaced by application of a physically reasonable electric-field strength (4). Voltage-dependent events in membranes may be quantitatively interpreted on this basis (5). In order to confirm such a mechanism, more direct experimental data are needed. Dielectric dispersion, i.e., the frequency dependence of dielectric constant and loss, provides information with regard to possible structural states and their dipolar properties as they occur in appropriate and clearly defined systems. Alamethicin seems to be specially well suited to be studied in this way. Its primary structure has been elucidated as being a certain linear sequence of 19 amino acids (6). From circular-dichroism spectra, pronounced changes of molecular conformation are indicated depending on the lipophilicity of the solvent (7). In hydrophilic media there is a comparatively low apparent α-helix content. This is drastically increased by material more similar to the amphiphatic constituents of a membrane. We have chosen a mixture of dioxane and *n*-octanol where (by varying the volume ratio of the pure solvents) structural change can be induced continuously.

Some similar dielectric data were already reported very recently for alamethicin in dioxane/ethanol (8). Our investigation, however, covers wider ranges of frequency as well as solvent composition and there will be a more detailed quantitative evaluation of molecular structure and dipole moments. In addition, octanol should approximate a membranelike medium better than ethanol.

2. MATERIAL AND METHODS

Alamethicin (R_F50) was purchased from the PHLS Centre for Applied Microbiology & Research, Wiltshire, England. After having prepared a stock solution in methanol the actual solutions to be investigated were eventually made as follows: We let an appropriate volume of the stock evaporate at 40°C and then redissolved the remaining solute in the desired solvent. Concentrations were determined from circular dichroism (CD) spectra recorded with a Cary 61 instrument using the data in the literature (7), which were found to be consistent with ours.

Regarding molecular weight of alamethicin in octanol a series of Yphantis-type equilibrium runs was carried out by means of a Beckman model E analytical ultracentrifuge (Beckman Instruments, Spinco Div.,

BIOPHYS. J. © Biophysical Society · 0006–3495/82/08/211/09 $1.00
Volume 39 August 1982 211–219

Palo Alto, CA) equipped with schlieren optics. (We are grateful to Mr. A. Lustig for his expert service in doing this work).

The dielectric dispersion measurements were performed on two impedance bridges manufactured by Boonton Electronics, Parsippany, NJ: a 75C direct-capacitance bridge covering 5–500 kHz and a 33A/1 admittance bridge for the range 1 to 100 MHz. We have checked the accuracy and reproducibility of these instruments with the aid of resistance and capacitance standards. Appropriate calibration charts were then used to correct the original values read on the scales.

Sample solutions were always measured at 25°C in a thermostatable cylindric dielectric cell with a volume capacity of about 0.75 ml (distance between the electrodes is <1 mm). Pure platinum, stainless steel and teflon were used for the material of the outer and inner electrodes and the insulating parts, respectively. Calibration with standard test substances such as carbon tetrachloride, benzene, chlorobenzene, and dichlorethylene resulted in a very good linear relationship between measured capacitance C and relative permittivity ϵ' (with an average deviation $|\Delta\epsilon'| < 0.019$ from the four references), namely

$$\epsilon' = 1 + 0.078_3\,(\text{pF})^{-1} \cdot (C - C_0)$$

(C_0 refers to the empty cell). Accordingly, the electric conductivity of the sample would be

$$\kappa = 6.9 \cdot 10^{-3}\text{cm}^{-1} \cdot G,$$

if G is the measured conductance. In addition we have confirmed this relation directly by calibration with dilute aqueous KCl. The dielectric loss can therefore be evaluated as

$$\epsilon'' = 1.24 \cdot 10^{-2}\,(\text{MHz}/\mu\text{S})\,[(G - G_0)/f]$$

(G_0 is the static conductance encountered at low frequencies and f the frequency of the applied voltage).

It must be noted that a lead inductance of $8.4 \cdot 10^{-9}$H was found for the connection between the high-frequency bridge and the cell. Thus, above 5 MHz, the values of G and C read from the instrument deviated from the true ones. Therefore, these read values were corrected by means of the pertinent quantitative expressions (9).

We have always evaluated measured data of the given solution together with those of the respective solvent (ϵ' was 10.04 for pure octanol, decreasing towards 2.31 for pure dioxane) and then determined the corresponding $\Delta\epsilon'$ from the difference of the C-values, thereby improving the relative accuracy of the dielectric increment contributed by the solute. Some dispersion of the solvent itself interferes with such procedure. It becomes significant at higher frequencies (i.e., at and above 10 MHz) in the case of pure octanol. This has been corrected for in the data given below.

3. EXPERIMENTAL RESULTS

A typical example of the dispersion observed for the $\Delta\epsilon'$ of alamethicin in pure octanol is presented in Fig. 1. The solid curve fitted to the measured points above about 50 kHz has been calculated on the basis of an ordinary Cole-Cole plot (10) as to be seen in Fig. 2. In other words, our data are quantitatively expressed in complex notation according to the relation

$$\Delta\epsilon' - i\epsilon'' = \frac{\Delta\epsilon_0}{1 + (if/f_0)^{1-\alpha}} + \Delta\epsilon_\infty \qquad (1)$$

(where $i = \sqrt{-1}$; $\Delta\epsilon_\infty$: high-frequency limit of $\Delta\epsilon'$). This yields three parameters of the system, namely:

(*a*) $\Delta\epsilon_0$, the total dielectric increment in the limit of low frequencies as compared with the value ϵ'_∞ obtained at high frequencies;

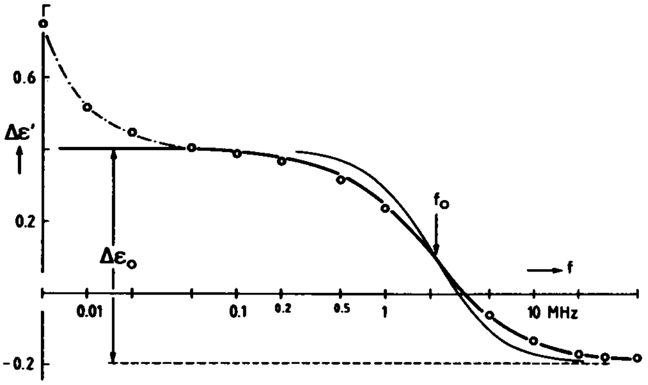

FIGURE 1 Dispersion of the dielectric increment $\Delta\epsilon'$ of alamethicin in pure octanol related to the dielectric constant of the solvent ($C = 2.1$ mg/ml, 25°C). The solid curve was calculated according to the Cole-Cole plot of Fig. 2*a*. The faint curve indicates the course of a dispersion described by a single relaxation time (i.e., Debye-type dispersion).

(*b*) f_0, the dispersion frequency at which $\Delta\epsilon' - \Delta\epsilon_\infty$ has decreased to one half of $\Delta\epsilon_0$ and ϵ'' reaches a maximum;

(*c*) α, a quantity reflecting the extent of a possible distribution of individual dielectric relaxation steps.

Eq. 1 is graphically equivalent to a circular arc when ϵ'' is plotted vs. $\Delta\epsilon'$ corresponding to the Cole-Cole plot in Fig. 2*a*. The difference between the two intercepts on the $\Delta\epsilon'$-axis equals $\Delta\epsilon_0$.

As shown by Fig. 1 there is a considerable increase of $\Delta\epsilon'$

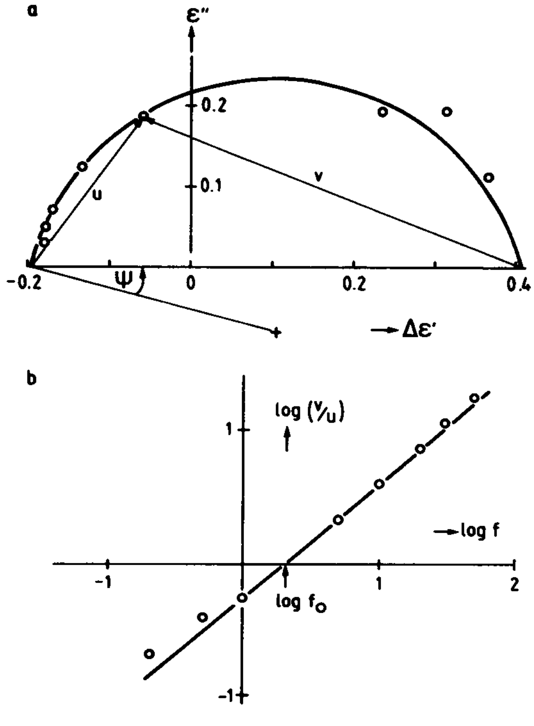

FIGURE 2 (*a*) Cole-Cole plot of the dielectric increment-loss data for the system of Fig. 1. The cross marks the center of the circle fitted to the measured points. From the angle Ψ the parameter α (see text) can be calculated as $\alpha = \Psi/90°$. (*b*) Linear plot of the data of part *a*, allowing determination of f_0 and α (see text).

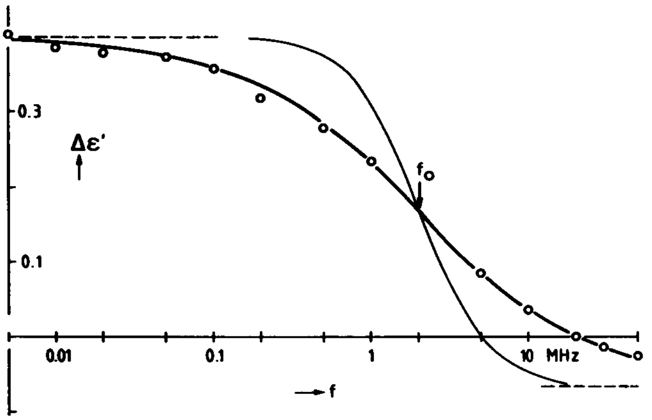

FIGURE 3 Dielectric dispersion of alamethicin in 36 vol % octanol/dioxane ($C = 4$ mg/ml, 25°C) as represented in Fig. 1.

at frequencies below 50 kHz. Apparently this is not caused by plain electrode polarization, since we did not find such an effect with dielectrically nondispersive test solutions of even much greater conductivity. On the other hand, it is quite uncertain which kind of rather slow polarization might be responsible. For the present we may leave this question out of the discussion.

The parameters f_0 and α are most conveniently determined using the distances u and v defined in Fig. 2*a*. It can be shown (10) that

$$\log(u/v) = (1 - \alpha)\{\log f - \log f_0\} \tag{2}$$

implying that the straight line in Fig. 2*b* intercepts the frequency axis at f_0 whereas its slope equals $1 - \alpha$.

A value of $\alpha = 0$ indicates the so-called pure Debye case associated with a single dielectric relaxation time. In Fig. 1 we have drawn a finer curve to represent the corresponding course of frequency dependence. Apparently only a comparatively small degree of broadening of the actually measured curve occurs.

Adding more and more dioxane to the octanol resulted in the disappearance of the additional low-frequency effect, a decay of $\Delta\epsilon_0$ (at fixed concentration), and greater α-values, reflecting a pronounced increase in the extent of broadening of the dispersion curve or, in other words, a wider distribution of relaxation times. A typical example is represented by the data in Figs. 3 and 4. Note that this case refers to a higher concentration of the peptide than the one in the figures discussed before. For a number of different solvent compositions (measured as percent by volume of octanol in the total original volume of the solvents) the dielectric parameters (i.e., f_0, $\Delta\epsilon_0$, α) have been determined as described.

Values of f_0 are assumed to be independent of peptide concentration (as was actually established in octanol). They change, however, with varying the octanol content as plotted in Fig. 5*a*. Under the simple assumption of a rotational mechanism of dipolar orientation (for more details see section 4.2) one should expect that

$$f_0 = kT/(\pi\bar{\zeta}_r) \tag{3}$$

(k, Boltzmann's constant; T, absolute temperature). The quantity $\bar{\zeta}_r$ stands for an appropriate friction coefficient of rotary motion, which can be expected to be proportional to the viscosity of the solvent, η, provided the dipolar structures remain invariant. Starting with the f_0-value observed at 100% octanol, the experimental points should then

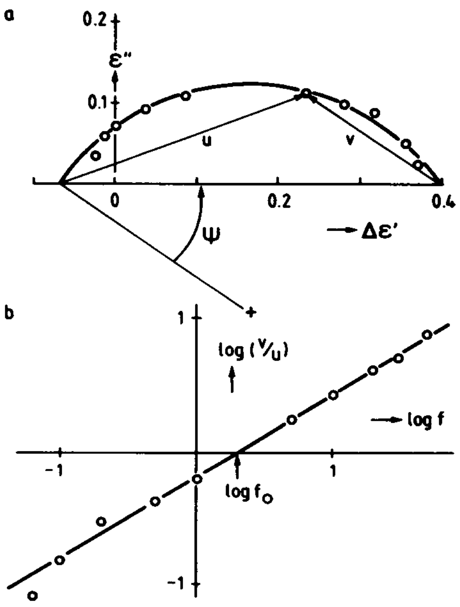

FIGURE 4 Data for the system of Fig. 3 plotted as in Fig. 2.

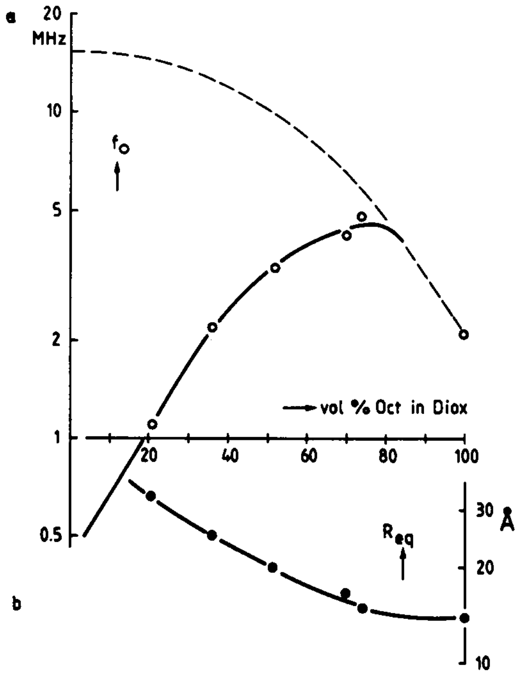

FIGURE 5 (*a*) Dispersion frequency f_0 as measured for various octanol contents of the solvent. The dashed curve is expected if the effect of viscosity alone is responsible for the change of f_0. (*b*) Radius of an equivalent spherical particle vs. octanol content.

follow the dashed curve (respective values of η were determined by means of Ubbelohde capillary viscosimeters). Evidently the actual results become drastically smaller as soon as the octanol content falls below 80%. The apparent increase of $\bar{\zeta}_r$ reveals an increase of the average size of the dipolar structures at higher portions of dioxane. With the $\bar{\zeta}_r$-value for spherical particles (= $8\pi\eta R^3$at a radius R), Eq. 3 can be used to calculate the radius of an equivalent sphere

$$R_{eq} = \{kT/(8\pi^2\eta f_0)\}^{1/3} \tag{4}$$

as given in Fig. 5*b*. Of course this has only a formal meaning (as long as we do not know that the particles are really spherical), but it nevertheless allows some estimate of molecular size and changes in it. In our case it obviously signals that there is indeed a considerable extension of particle dimensions when the solvent becomes more and more enriched with dioxane.

The solvent dependences of our $\Delta\epsilon_0$ and α are shown by Figs. 6*a* and *b*, respectively. All indicated results have actually been measured at an alamethicin concentration of 4 mg/ml except for the one referring to pure octanol. Regarding the latter we have studied a greater number of different concentrations. The respective $\Delta\epsilon_0$ have been recorded in Fig. 7. The value interpolated for 4 mg/ml was entered in Fig. 6*a*. As far as f_0 and α are concerned we did not find any significant effect of concentration.

Finally we report that the ultracentrifugation work in pure octanol yielded a weight-average molecular weight of 2,700 using a partial volume of $\bar{v}$ = 0.80 ml/g (as determined from pertinent density measurements).

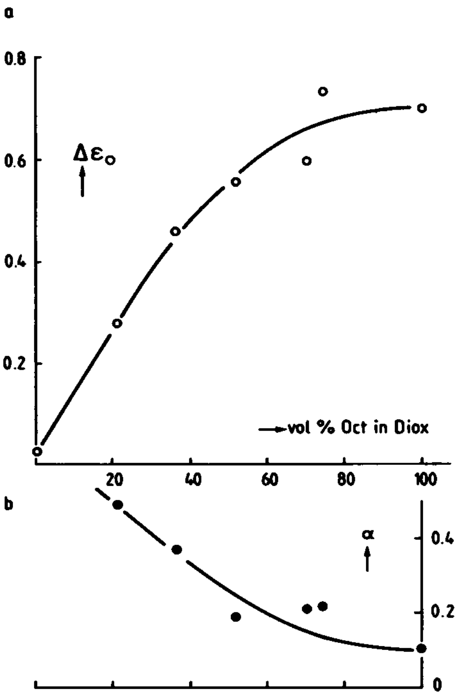

FIGURE 6 Dependence on octanol content as reflected by (*a*) the static dielectric increment $\Delta\epsilon_0$ and (*b*) the spectral distribution parameter α.

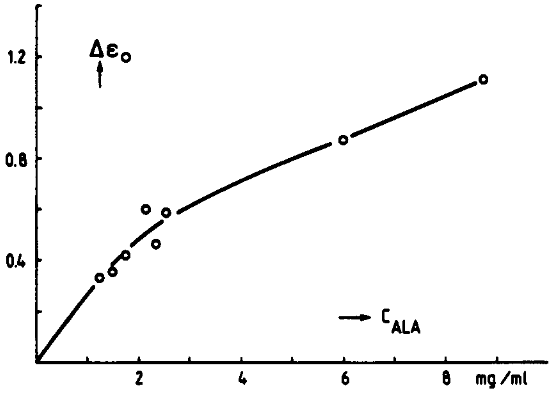

FIGURE 7 Concentration dependence of $\Delta\epsilon_0$ in pure octanol (25°C).

The molecular weight of an alamethicin monomer is 1,962, as can be computed on the basis of its chemical composition (6). Therefore the peptide must be predominantly monomeric in octanol with only some minor portion of dimers and/or larger aggregates. According to the diagrams of Figs. 5 and 6, this structural constellation appears to remain unaltered when smaller amounts of dioxane are added so that at least about 80% octanol is retained. Increasing the dioxane content beyond that point clearly induces more and more aggregation as reflected by the decrease of f_0. The increase of α, on the other hand, must be qualitatively interpreted as evidence of gradually rising polydispersity of the aggregates. From the decay of $\Delta\epsilon_0$ we gather that the average effective dipole moment per monomer in such aggregates eventually approaches almost zero.

4. QUANTITATIVE DISCUSSION

4.1 Monomer Content in Pure Octanol

Naturally we must start out from the hypothesis that a polydispersity of molecular structures of alamethicin may exist in any of the diverse solutions. Possibly there are one or even more monomeric conformations as well as all kinds of aggregates of these. As far as the total monomer content is concerned we can deduce at least a lower bound from determinations of an apparent molecular weight. With a mass fraction of monomer, $y_1 = C_1/C$ (C_1, C: mass per volume of the monomer form[s] and of total solute, respectively), the weight-average molecular weight, M_w, becomes

$$M_w = y_1M_1 + (1 - y_1)nM_1 \tag{5}$$

(M_1, monomer molecular weight) provided we assume for the sake of simplicity that, in addition to the monomers, only aggregates of n monomers occur.

Inserting our present values of M_w(= 2,700) and M_1(= 1,962) we find y_1 = 0.62 if a monomer-dimer system is supposed. This is indeed a lower bound of the monomer mass fraction since for any other possible distribution of aggregate sizes, y_1 must evidently be greater. In particular, with only one kind of aggregate, we find $y_1 = 0.81$ if $n = 3$, $y_1 = 0.93$ if $n = 6$.

4.2 Dispersion Frequency and Molecular Dimensions

So far we have no reason to doubt that dielectric dispersion is simply caused by the finite rate of rotational motion of permanent dipoles on the alamethicin monomers and aggregates when these orient in the applied electric field. A certain particle rotating about one of its principal axes of inertia is described by a relaxation time[1]

$$\tau = \zeta_r/(2kT) \tag{6a}$$

involving a rotary frictional coefficient ζ_r, which equals the product of solvent viscosity and a factor that depends on shape, size, and axis of rotation. For rigid particles shaped as spheroids (i.e., ellipsoids of revolution) pertinent expressions of ζ_r are available from hydrodynamic theory (11).

We shall therefore approximate our dipolar particles by such spheroids. These are described in terms of the two semi-axes, a and b, the first one refers to the axis of symmetry and the second one is perpendicular to it. Let us assume that all particles are the same and the dipole moment is parallel to one of these axes. This implicates a single dielectric relaxation time (equivalent to $\alpha = 0$) and a corresponding dispersion frequency

$$f_0 = 1/(2\pi\tau) = \frac{kT}{8\pi^2\eta a^3}\phi^*(p) \tag{6b}$$

where $\phi^*(p)$ stands for an explicit function of the axial ratio $p = a/b$. There are four different cases with respective specific $\phi^*(p)$, depending on whether $p > 1$ (prolate spheroids) or $p < 1$ (oblate spheroids), and whether the dipole is oriented in the direction of the axis of symmetry or perpendicular to it. At any rate we have $\phi^*(p) \longrightarrow 1$ for $p \longrightarrow 1$ in accordance with Eq. 4. A second experimentally accessible quantity determined by the parameters a and p may thus be combined with Eq. 6 in order to evaluate these structural parameters. Most simply we may take advantage of the particle volume

$$v_0 = \frac{4\pi}{3}ab^2 = \frac{4\pi}{3}a^3/p^2. \tag{7}$$

By means of this relation we eliminate a^3 in Eq. 6 and obtain

$$f_0 = \frac{kT}{6\pi\eta v_0}\phi(p) \tag{8a}$$

with $\phi(p) = \phi^*(p)/p^2$. Considering the molar mass of the particle, M, and the appropriate partial specific volume, $\bar{v}$, we set

$$v_0 = \gamma_s \cdot \frac{M}{N_A}\bar{v} \tag{8b}$$

(N_A, Avogadro's number) where γ_s is a factor that takes into account that the actual particle volume may deviate somewhat from the apparent one because of solvation effects.

By means of Eq. 8 the axial ratio can be determined when experimental data of f_0 and v_0 are available. Based on the pertinent expressions for ζ_r in the original publication (11), the individual versions of $\phi(p)$ are graphically presented in Fig. 8. Once p is known, Eq. 7 lets one calculate both semi-axes separately. For a prolate spheroid we find

$$\phi(p) = \frac{3}{2} \cdot \frac{p^2}{p^4 - 1} \cdot \left[\frac{2p^2 - 1}{p\sqrt{p^2 - 1}} \ln(p + \sqrt{p^2 - 1} - 1\right] \tag{9a}$$

for a dipole parallel to the axis of symmetry. The function is approximated well by

$$\phi(p) = 3 \cdot (\ln p + 0.193)/p^2 \qquad (\text{if } p > 2). \tag{9b}$$

Apparently this $\phi(p)$ falls drastically below unity when p increases. Should the dipole point in a direction perpendicular to the axis of symmetry,

$$\phi(p) = \frac{3}{2} \cdot \frac{p^2}{p^2 - 1} \cdot \left\{1 - \frac{1}{p\sqrt{p^2 - 1}} \ln(p + \sqrt{p^2 - 1})\right\} \tag{10}$$

applies. As illustrated in Fig. 8 the $\phi(p)$ now increases above unity, but only to a rather small extent, eventually approaching 1.5 at large p.

4.3 Examining Our Experimental f_0 Data

Since the aggregation pattern, the distribution of permanent dipoles over the diverse aggregates, as well as the effect of solvation on particle volume are not known so far, application of the above theoretical relations requires some basic assumptions before we can calculate the dimensional parameters of the dipolar particles. Let us, therefore, explore a number of different possibilities.

When taking advantage of the Eq. 8, it generally follows for an aggregate of n monomers in 100% octanol (at 25°C where $\eta = 8.64$ cP) that

$$\phi(p) = 0.103\, n\gamma_s(f_0/\text{MHz}). \tag{11}$$

---

[1] Hill, N. E., W. E. Vaughan, A. H. Price, and M. Davies. 1969. Dielectric Properties and Molecular Behaviour. Van Nostrand Reinhold Company, New York: p. 60 ff.

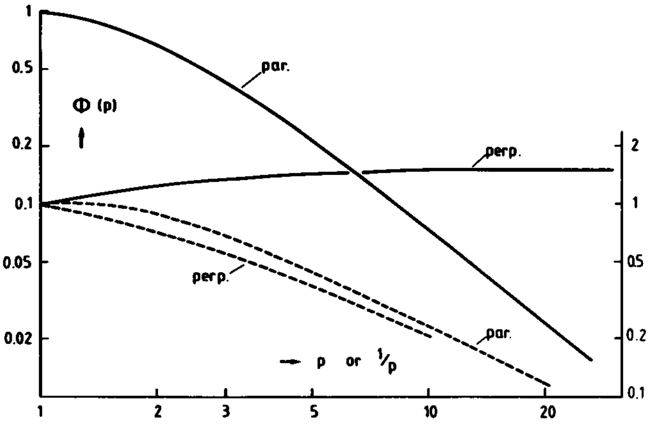

FIGURE 8 The function $\phi(p)$ of Eq. 8a as it depends on the axial ratio p. The solid curves refer to the case $p > 1$ and dipoles directed parallel and perpendicular to the symmetry axis (left ordinate scale, parallel; right one, perpendicular). The dashed curves apply to $p < 1$ (right scale for both).

As must be emphasized, however, this f_0 refers to a pure Debye dispersion curve associated with the dipole directed either parallel or perpendicular to the symmetry axis. After p has been determined, a (and b) can be computed by means of the relation

$$a = 8.54(n\gamma_s p^2)^{1/3}\text{Å}, \tag{12}$$

which is derived from Eqs. 7, 8b.

A first (but rather extreme) possibility would be that measurable dipoles are carried only by monomeric structures. The observed frequency dependence then solely reflects rotary diffusion of these particles. With $f_0 = 2.1$ MHz (which has previously been evaluated from the data of Fig. 1) and $\gamma_s = 1$ (i.e., assuming no solvation effect), Eq. 11 immediately yields $\phi(p) = 0.21$. For a prolate spheroid with the dipole parallel to the axis of symmetry the respective ϕ-curve in Fig. 8 leads to an axial ratio of $p = 5$. Employing Eq. 12 we then obtain $a = 25$ Å, $b = 5$ Å. Accordingly the "length" and "diameter" become 50 Å and 10 Å, respectively. This appears to be an unlikely elongated and thin shape (even some solvation effect does not essentially improve the situation). A dipole predominantly oriented perpendicular to the symmetry axis can be excluded because this requires $\phi(p) > 1$. Oblate spheroidal form, on the other hand, will be disregarded owing to the unreasonably small values of a (≈ 2 Å) that would be associated with it.

Returning to the prolate shape we note that the assumption of a dipole exactly parallel to the symmetry axis does not explain the obvious broadening of the dispersion curve as compared with the pure Debye form (i.e., one described by $\alpha = 0$). Under the assumption that all dipolar particles have indeed the same size and shape, this can only be interpreted as due to some extra dipolar component perpendicular to the symmetry axis. The measured dispersion curve would then be caused by two Debye curves superimposed on each other, reflecting rotation of the parallel and perpendicular dipole components, respectively. It turns out that, actually, no satisfactory fit of the experimental curve can be achieved in this way, apart from the implication that the particle would exhibit an even more extreme axial ratio than before.

Because of these arguments, we must definitely take into account appreciable dipolar contributions by the aggregates. At least two Debye terms of comparable amplitudes are required so that

$$\Delta\epsilon' = \left[\frac{\beta}{1 + (f/f_{01})^2} + \frac{1-\beta}{1 + (f/f_{0n})^2}\right]\Delta\epsilon_0 + \Delta\epsilon_\infty \tag{13}$$

attributing the first term to the monomer species and the second one to aggregates of n monomers. Indeed this allows rather good fits of the experimental curve in Fig. 1 for β around 0.5. The best result is obtained with

$$\beta = 0.61, \qquad f_{01} = 3.9 \text{ MHz}, \qquad f_{0n} = 0.76 \text{ MHz}.$$

The quite reduced value of f_{0n} necessarily implies that some fairly large polar particles exist. These can only be aggregates since for a monomer particle with such a low f_0, an extremely unreasonable elongated shape is deduced.

Inserting this f_{01} for f_0 in Eq. 11, one obtains $\phi(p) = 0.40\gamma_s$. Solvation effects described by the factor γ_s may be caused by solvent volume contraction (due to denser packing) and/or increased effective particle volume due to binding of solvent molecules (e.g., one octanol molecule rigidly attached to an alamethicin monomer would enlarge it by about 8%). To assess the significance of this point, we inspect the dimensional parameters of the monomer particles, which result in case of 0 and 20% greater volume than indicated by $\bar{v}$:

$$\text{if } \gamma_s \begin{cases} = 1.0 \\ = 1.2 \end{cases} \text{then } p \begin{cases} = 3.15 \\ = 2.7 \end{cases} a \begin{cases} = 18.4 \text{ Å} \\ = 17.6 \text{ Å} \end{cases} b \begin{cases} = 5.85 \text{ Å} \\ = 6.5 \text{ Å}. \end{cases}$$

Assuming $n = 2$, analogous evaluations of f_{0n} yield for dimeric aggregates

$$\text{if } \gamma_s \begin{cases} = 1.0 \\ = 1.2 \end{cases} \text{then } p \begin{cases} = 6.2 \\ = 5.5 \end{cases} a \begin{cases} = 36.2 \text{ Å} \\ = 35.6 \text{ Å} \end{cases} b \begin{cases} = 5.85 \text{ Å} \\ = 6.5 \text{ Å}. \end{cases}$$

Choosing $n = 3$ and 6, respectively, and $\gamma_s = 1.2$ we note as the resulting dimensional parameters of trimers and hexamers,

$p = 4.1$; $a, b = 33.6, 8.15$ Å, and

$p = 2.35$; $a, b = 29.1, 12.4$ Å.

Similar considerations regarding the situation in octanol mixed with dioxane are not possible at the present time. For one thing we lack data allowing evaluation of an average particle mass. On the other hand, the comparatively large α-values at higher dioxane content indicate a rather wide distribution of aggregate sizes. Therefore the observed f_0 must be taken as some mean over a broad spectrum of individual Debye-type f_0. Nevertheless we can at least estimate the approximate average aggregation number of dipolar particles.

For instance, at 21% octanol (where η = 1.35 cP) we found a f_0 of 1.1 MHz which would yield $\phi(p) = 0.018\, n\gamma_s$. Extremely unreasonable elongated shapes are then obtained with $n < 10$. More likely axial ratios in the range of $p = 2 - 0.5$ require aggregation numbers of 35 to about 50 (the larger bound referring to spherical micelles having a radius of 33 Å). On the other hand, much greater numbers can definitely be excluded because they are clearly not consistent with the measurements.

4.4 Dielectric Increment and Dipole Moments

Rotatable solute particles with a permanent dipole moment μ_j contribute to the overall dielectric constant of the solution. In principle, it should therefore be possible to calculate μ_j from the respective dielectric increment, $\Delta\epsilon_{0j}$, measured as a corresponding part of $\Delta\epsilon_0$, the difference between the levels of ϵ' at low and high frequencies. Unfortunately there is no generally useful theory to do this in a rigorous way. However, on the basis of the Onsager-Debye approach (13) we obtain a relation which can be expected to approximate reasonably well the experimental results in the case of sufficient dilution of the solute, namely

$$\Delta\epsilon_{0j} = g_j \frac{\mu_j^2}{3\epsilon_v kT} N_A (C_j/M_j) \qquad (14)$$

($\epsilon_v = 8.85 \cdot 10^{-12}$ F/m, absolute permittivity of vacuum) where C_j stands for the mass per volume concentration of the particles in question (M_j, molar mass) and g_j denotes a factor that takes into account the effect that the acting local fields deviate from the externally applied one. For a dipole moment directed along a principal axis of an ellipsoidal body we have (12)

$$g_j = \frac{\epsilon[\epsilon - (\epsilon - 1)A_j][1 + (\epsilon_0 - 1)A_j]^2}{[\epsilon - (\epsilon - \epsilon_0)A_j]^2}. \qquad (15)$$

This involves the low-frequency dielectric constant of the system, ϵ, and the "optical" dielectric constant of the material of the particle, ϵ_0. In addition, there is a shape factor, A_j, depending on the axial ratios. In the special case of a prolate spheroid it can be shown (13) that parallel to the axis of symmetry

$$A_\| = \frac{1}{2p^2e^3}\left[\ln\frac{1+e}{1-e} - 2e\right] \text{where } e = \sqrt{1-p^2}, \qquad (16)$$

and perpendicular to it

$$A_\perp = (1 - A_\|)/2. \qquad (17)$$

This implies $A = 1/3$ if we deal with a spherical particle and

$$\left.\begin{aligned} A_\| &\approx \{\ln(2p) - 1\}/p^2 \\ A_\perp &\approx 1/2 \end{aligned}\right. \quad \text{if } p > 5$$

Accordingly we find $g_\| \rightarrow 1$ when $p >> 1$.

4.5 Calculation of Dipole Moments

Let us consider the case of alamethicin dissolved in pure octanol. As has been pointed out above, the observed dispersion curve cannot be caused by dipole moments associated solely with the monomers.

Assuming again n-mers in addition to monomers it follows from Eq. 14 that

$$\Delta\epsilon_0 = \left\{g_m y_1 + g_a \frac{(1 - y_1)}{n}\left(\frac{\mu_n}{\mu_1}\right)^2\right\} \frac{N_A C}{3\epsilon_v M_1 kT}\mu_1^2 \qquad (18)$$

(g_m, g_a are the g-factors of the monomer and aggregate, respectively). The fraction contributed by the monomers, β, may thus be calculated according to the relation

$$1/\beta = 1 + (g_a/g_m)\frac{1 - y_1}{n y_1}\left(\frac{\mu_n}{\mu_1}\right)^2. \qquad (19)$$

This β is of course identical with the parameter introduced already in Eq. 13.

First we examine the possibility of dimeric aggregates (implying $y_1 = 0.62$). With $\epsilon = 10.5$, $\epsilon_0 = 2.5$, and the p-values derived in section 4.3, Eqs. 15 and 16 yield g_m = 1.42 or 1.52, g_a = 1.16 or 1.19, depending on the solvation factor γ_s being 1.0 or 1.2, respectively. With $\beta = 0.61$ it follows that $\mu_2/\mu_1 = 1.60$ or 1.63. The dipole moment of the monomer calculated by means of Eq. 18 then comes out as μ_1 = 80 or 77 D (D, Debye units). Analogous considerations with trimers lead to values of μ_3/μ_1 that are >3. This means that the dipole moment per monomer would increase upon aggregation. The same effect is encountered for higher aggregates.

As far as the alamethicin aggregates in the dioxane enriched solvent mixtures are concerned we can only give estimates of an average dipole moment. Turning to the case of 21% octanol by volume and assuming a spherically shaped micelle Eq. 14 yields a dipole moment of 235 D (using a g-factor of 2.0 as derived for $\epsilon = 3.2$). Since we have argued above that the aggregation number should be about 50 this is equivalent to only an effective 5 D per monomer.

4.6 Relevant Literature Data

As was already mentioned in the introduction, dielectric dispersion of alamethicin has recently been studied in a similar solvent mixture, namely dioxane and ethanol (covering a frequency range from 0.5 to 50 MHz) (8). Qualitatively the results are similar to ours. At the lowest ethanol content ($\approx 10\%$) f_0 and $\Delta\epsilon_0$ were reported to be comparatively small (≈ 10 MHz and ≈ 0.08 per mg/ml, respectively). These quantities increased with higher ethanol content, apparently reaching a constant level at about 50% ethanol: $f_0 \approx 50$ MHz and $\Delta\epsilon_0 \approx 0.2$ per mg/ml. No data for greater percentages of ethanol have been given, however.

The finding that the dispersion occurs at much higher frequencies than observed in our system can at least in part be explained by the fact that the viscosity of dioxane/ethanol mixture ($\eta \approx 1.2$ cP) is considerably smaller than that of octanol. Adjusting Eq. 11 to the present case yields

$$\phi(p) = 0.014\, n\gamma_s(f_0/\mathrm{MHz}) \qquad (20)$$

(with $\bar{v} = 0.82$ ml/g as measured in 100% ethanol [14]). Molecular weight determinations in pure ethanol clearly indicated the exclusive presence of monomers (14). The conjectural independence of f_0 and $\Delta\epsilon_0$ down to 50% ethanol in dioxane would accordingly suggest that only monomers exist even in this solvent mixture. After inserting the appropriate n and f_0 as well as $\gamma_s = 1$ in Eq. 20, the approach introduced above leads to $p = 1.9$, $a = 13.1$ Å, $b = 6.9$ Å.

It must be emphasized, however, that the dispersion curve in question also exhibits some deviation from a pure Debye course. This system, too, must therefore be described by at least two individual superimposed Debye relaxation terms. Since we have excluded aggregates, these would have to be attributed to the rotations of dipolar components parallel and perpendicular to the axis of symmetry. Let us assume for instance, that $p = 2.5$ ($a = 15.7$ Å, $b = 6.3$ Å). This would be associated with Debye curves involving $f_0 = 38$ MHz (parallel mode) and 95 MHz (perpendicular mode) allowing an improved fit of the dispersion curve. Accordingly the dimensions of the particle may well be largely the same as those evaluated for the octanol case, provided that there is a comparatively small perpendicular component of the dipole. Calculation of the monomer dipole moment using Eq. 14 results in a value of about 65 D.

4.7 Conclusions

A number of rather definite points can be deduced now for alamethicin in pure octanol. From the arguments in section 4.1, it follows that at least about two-thirds of the solute exists as single monomers. Nevertheless there must be an appreciable amount of quite polar aggregates. If we would attribute the observed dielectric dispersion curve largely to the monomers, these must have an unreasonably extended shape and a large dipole moment much greater than 100 D, which is unlikely. In addition, no satisfactory fit of the frequency dependence would be possible, not to mention the pronounced inconsistence with results for the dioxane/ethanol solvent. Even more such difficulties are encountered if we assume that essentially only the aggregates are polar, but the monomers are not.

We infer from these considerations that at least two individual f_0 values must be considered with the larger one (about 4 MHz) to be attributed to rotation of the monomeric dipoles. Taking into account up to 20% solvation effect, this yields a particle length of 36 Å and a diameter of 12 Å, which is in excellent agreement with a model proposed some years ago (15). There is some evidence that about 40% of the alamethicin may be α-helical (7, 16). This α-helical portion would be about 12 Å long and have a diameter of 13 Å. Thus the dimensions of the whole molecule would comply quite well with our results, provided that the nonhelical portion is somewhat more extended than the helical one (as can be expected).

The other f_0 value (which turned out to be distinctly smaller than 1 MHz) had to be attributed to the rotary movement of aggregate dipoles. The size of these aggregates, however, cannot be assessed on the basis of such an f_0 alone. Therefore we refer to the argument in section 4.5 with regard to the contribution of aggregate dipoles to $\Delta\epsilon_0$. It indicated that for pure n-mers and $n \geq 3$ the dipole moment per monomers would have to increase upon aggregation. This requires conformational changes to a state of higher polarity in the aggregates, which appears to be rather unlikely. Hence we may conclude that mainly dimers are formed. Recalling the dimensional parameters evaluated in section 4.3, we note that these dimers must be about twice as long as a monomer and have practically the same diameter. Considering in addition that $\mu_2 > \mu_1$, a "head-to-tail" dimerization process is apparently indicated.

At this point it should be emphasized that our discussion has been based so far on a superposition of only two Debye terms, serving as a first approximation. Now it seems reasonable to introduce a somewhat more complex structural background. First the direction of the dipole in the monomer may deviate slightly from the long axis so that an additional, though small Debye term involving a comparatively high f_0 appears to be in compliance with our approach regarding the dioxane/ethanol case examined in the preceding section. Second, a head-to-tail dimerization as suggested by our octanol data must naturally not be expected to stop at dimeric aggregates. Under the given circumstances some portion of appropriate higher aggregates may be present leading to Debye terms with low f_0 and small amplitudes. This more realistic approach tends to increase the number of adjustable parameters allowing an even better fit of the experimental data. It leads to slightly smaller values of a and μ_1, and somewhat greater b and μ_2/μ_1.

Summarizing the essentials of our analysis, we note that in octanol the alamethicin may exist as a monomer particle of about 35 Å in length and 13 Å in diameter, with a dipole moment of about 75 D directed nearly parallel to the long axis. Dimers can be formed by linking monomers head to tail. At the concentrations (of a few milligrams per milliliters) usually employed in this investigation, primarily monomers occur. The rest of the solute material, however, is largely present as dimers.

Aggregation in the dioxane-enriched solvent mixtures would certainly proceed in a different way. The obvious decay of apparent helix content (only 18% in pure dioxane (7)) indicates that there is another less polar conformational state of the aggregated monomers. We may therefore propose a second monomer structure of low dipole moment that easily forms larger aggregates but becomes more and more unstable when the lipophilicity of the medium increases.

This work was supported by grant nos. 3.099-77 and 3.545-79 from the Swiss National Science Foundation.

Received for publication 12 August 1981 and in revised form 13 November 1981.

REFERENCES

1. Mueller, P., and D. O. Rudin. 1968. Action potentials induced in biomolecular lipid membranes. *Nature (Lond.).* 217:713-719.
2. Boheim, G., and H. A. Kolb. 1978. Analysis of the multi-pore system of alamethicin in a lipid membrane. I. *J. Membr. Biol.* 38:99-150.
3. Cole, K. S. 1968. Membranes, Ions and Impulses. University of California Press, Berkeley.
4. Schwarz, G. 1977. Chemical transitions of biopolymers induced by an electric field and their effects in dielectrics and birefringence. *Ann. N. Y. Acad. Sci.* 303:190-197.
5. Schwarz, G. 1978. On the physico-chemical basis of voltage-dependent molecular gating mechanisms in biological membranes. Quantitative analysis of activation and inactivation of asymmetry currents in biological membranes, based on a conformational transition model. *J. Membr. Biol.* 43:127-167.
6. Gisin, B. F., S. Kobayashi, and J. E. Hall. 1977. Synthesis of a 19-residue peptide with alamethicin-like activity. *Proc. Natl. Acad. Sci. U. S. A.* 74:115-119.
7. Jung, G., N. Dubischar, and D. Leibfritz. 1975. Conformational changes of alamethicin induced by solvent and temperature. *Eur. J. Biochem.* 54:395-409.
8. Yantorno, R. E., S. Takashima, and P. Mueller. 1982. Dipole moment of alamethicin as related to voltage-dependent conductance in lipid bilayers. *Biophys. J.* 38:105–110.
9. Schwan, H. P. 1963. Determination of biological impedances. *In* Physical Techniques in Biological Research. W. L. Nastuk, editor. Academic Press, Inc., New York. 323-409.
10. Smyth, C. P. 1955. Dielectric Behavior and Structure. McGraw-Hill: p. 68 ff.
11. Gans, R. 1928. Zur Theorie der Brownschen Molekularbewegung. *Ann. Phys.* 86(4):628-656.
12. Böttcher, C. J. F. 1973. Theory of electric polarization. Vol. I. Elsevier/North-Holland, Amsterdam. 181 ff.
13. Stratton, J. A. 1941. Electromagnetic Theory. McGraw-Hill. 207 ff.
14. McMullen, A. I., and J. A. Stirrup. 1971. The aggregation of alamethicin. *Biochim. Biophys. Acta.* 241:807-814.
15. Baumann, G., and P. Mueller. 1974. A molecular model of membrane excitability. *J. Supramolec. Struct.* 2:538-557.
16. Butters, T., P. Hütter, G. Jung, N. Pauls, H. Schmitt, G. M. Sheldrick, and W. Winter. 1981. Zur Struktur des helikalen *N*-terminus im Alamethicin–α-Helix oder 3_{10}-Helix? *Angew. Chem.* 93: 904–905.